Environ. Sci. Technol. **2006**, *40,* 4672−4679

Study of the Interaction of Ni^{2+} and Cs^{+} on MX-80 Bentonite; Effect of Compaction Using the "Capillary Method"

G. MONTAVON,* E. ALHAJJI, AND B. GRAMBOW

Subatech Laboratory, UMR 6457, 4, rue Alfred Kastler, BP 20722, F-44307 Nantes Cédex 03 France

The goal of the paper is to assess the applicability of sorption models to describe the retention of contaminants on clay materials, both in dispersed and compacted states. A batch method is used to characterize the sorption equilibria between Cs, Ni, and MX-80 bentonite for solid-to-liquid ratios varying from 0.5 to 4200 kg/m^3. For compacted bentonite (dry density of 1100 kg/m^3), a new method is presented where the material compaction is performed in PEEK capillaries. Sorption edges and isotherms were measured in the presence of a synthetic groundwater. A model considering cation exchange reactions with interlayer cations and surface complexation reactions with edge sites was used for the dispersed state. Montmorillonite was shown to be the dominant interacting phase in MX-80 bentonite. The applicability of the model to compacted bentonite was tested. The results indicate that under conditions where the cation exchange mechanism is dominant, there is no difference between the dispersed and compacted states. For the degree of compaction studied, all exchange sites are available for sorption. For Ni, when surface complexation is the dominant sorption mechanism, a decrease of the Kd values by a factor of about 3 was observed (pH 7−8, trace concentrations). This could be explained quantitatively by a diminution of the conditional interaction constant between Ni and the edge surface site in the compacted state. One consequence of this decrease is that the contribution of the organic matter content of MX-80 bentonite to the total sorption becomes significant.

Introduction

Bentonite is a clay-based natural material which may serve as an engineered barrier in deep geological repositories for radioactive waste (e.g., ref *1*). The transport of contaminants in water-saturated porous clay systems is controlled by sorption (e.g., refs *2*, *3*). This interaction is typically modeled based on sorption data obtained from batch sorption measurements performed with dispersed bentonite, i.e., on systems with low solid-to-liquid (S/L) ratios. The literature on sorption of contaminants on dispersed bentonite is voluminous (e.g., refs *2*, *3*).

It is necessary to ensure that sorption parameters obtained on dispersed materials are able to describe the sorption processes in compacted media. This appears notably necessary for high degrees of compaction where the notion of free water is no longer valid (*4*) (i.e., for a dry density above 1700 kg/m^3). The experimental retention data in the compacted state (for dry densities varying from 400 to about 1800 kg/m^3) are generally determined indirectly, i.e., from migration studies (*3*, *5*−*8*). The comparison with the results obtained with dispersed bentonite shows that material consolidation has, in some cases, no effect on retention, in other cases it has a positive (increase of the retention) or negative (decrease of the retention) effect (3, *5*−*10*). The origin of the effect appears unclear; either the transport or the retention model is criticised (2−*7*, *9*, *10*). For the retention model, site accessibility is proposed as an explanation (*9*).

To better understand the relation between the retention of contaminants in dispersed and compacted sytems, it appears important to develop new methodologies to measure sorption data directly on compacted materials (*9*).

In this paper, a batch method allowing the characterization of the sorption equilibria between the contaminants and bentonite for high solid/liquid ratios is presented. The consolidation has been realized within capillaries. The low mass of bentonite used in the capillary allows us to change easily the experimental conditions. The method is applied to Cs and Ni with MX-80 bentonite for a S/L ratio of 4200 kg/m^3. pH edges and isotherms measured in the presence of a synthetic groundwater are compared with those measured in the dispersed state (S/L = 0.5−10 kg/m^3). The results were modeled based on published models obtained with pure clay materials (*11*−*13*). The effect of secondary phases on the total retention was discussed.

Materials and Methods

Materials. All chemicals used were of analytical purity. MX-80 bentonite was used without any purification, except for some sorption tests realized with Ni in the dispersed state, where bentonite was treated with H_2O_2 (S/L = 10 kg/m^3; NaCl 0.05M; H_2O_2 12%, T = 70 °C; five treatments) to selectively remove organic matter (*14*). The montmorillonite fraction amounts to 84% (*11*). Natural Ni and Cs were found in MX-80 bentonite with amounts of 5.4 mg/kg and 0.11 mg/kg, respectively (*15*). Experiments performed under acidic conditions (pH 2.5, $NaNO_3$ 0.05M) showed that about 65% of the inventories of Cs and Ni were mobilizable (*15*). A water content of 8% was determined by drying at 105 °C for 12 h and taken into account for the calculation of the bentonite concentration in the dispersed state. HTO, ^{63}Ni, and ^{137}Cs (with carrier) were obtained from CERCA−FRAMATOME, AMERSHAM, and CEA/DAMRI, respectively. Capillaries in PEEK of 1 mm internal diameter were used for the experiments realized with compacted bentonite.

Sorption Study. All experiments were performed at T = 23 ± 3 °C. Sorption data were measured using a typical water composition of the claystone of the Bure site (see Table 1). Two types of data sets were collected: in the first case, sorption is studied at initial fixed metal ion concentration as a function of pH (sorption pH edges) and in the second case, sorption was measured as a function of metal ion concentration at constant pH (sorption isotherms). For the measurement of pH edges, the pH value was varied between 4 and 9 using NaOH and $HClO_4$ stock solutions. For fixing the pH above a value of 4 for sorption studies, MES (2-(N−morpholino)ethane-sulfonic acid), MOPS (3-(N−morpholino)propane-sulfonic acid), and/or TRIS (tris(hydroxymethyl)-aminomethane) buffers at a concentration of 2×10^{-3}M were used. They are known to not alter the sorption behavior of metal ions on clay materials in the dispersed state (*12*). Some

* Corresponding author phone: +33 251 858 420; fax: +33 251 858 452; e-mail: montavon@subatech.in2p3.fr.

10.1021/es052483i CCC: $33.50
Published on Web 07/01/2006

TABLE 1. Analysis of the Equilibrium Conditions

		major cations (In mM)				minor ions (In μM)		
state	pH[a]	K	Ca	Na	Mg	Si	Al	Fe
consolidated state	4−9	0.6 ± 0.2	6.6 ± 1.1	57 ± 20	4.4 ± 0.7	107 ± 43	0.28 ± 31	<0.9
dispersed state	4−9	0.4 ± 0.1	5.9 ± 0.4	37 ± 8	3.0 ± 0.7			

[a] For pH > 7.8, experiments are performed in an inert athmosphere.

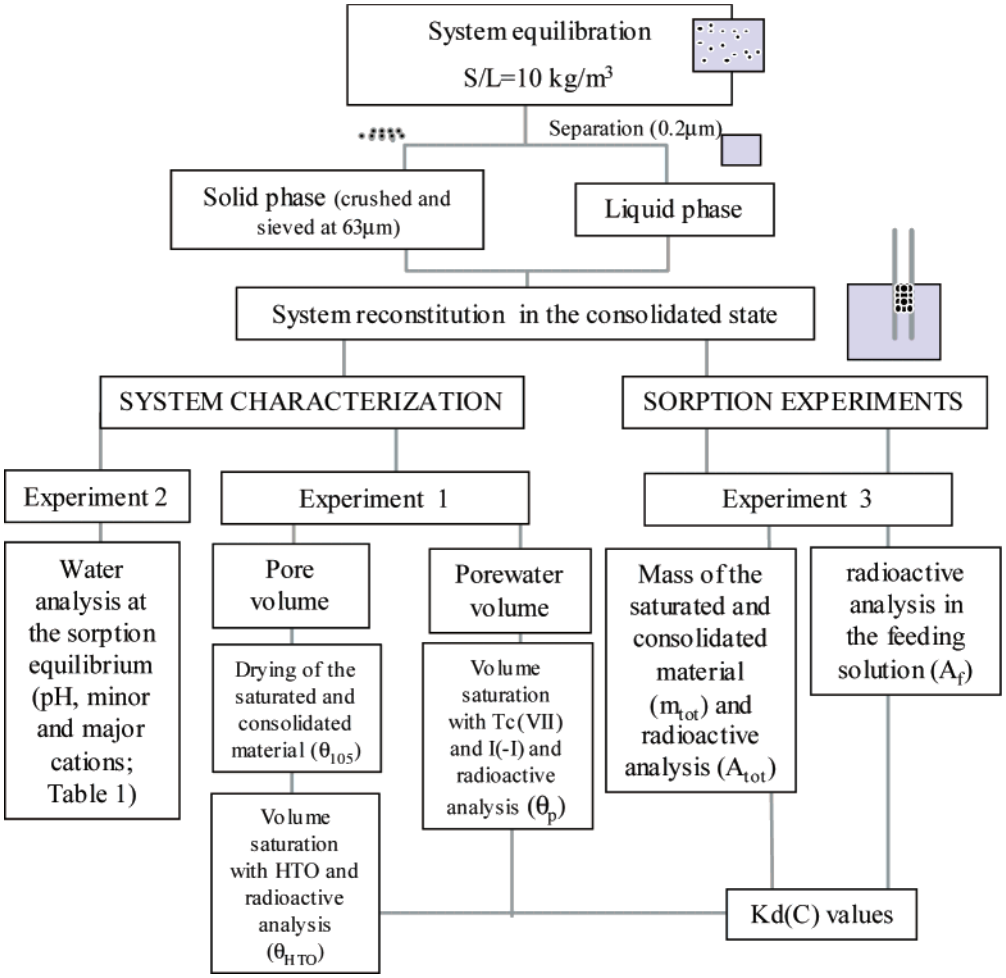

FIGURE 1. Description of the procedure followed to measure the retention data in the compacted state.

complementary experiments without buffers were performed for Ni to confirm the nonaffect in the compacted state. It was checked (in both consolidated and dispersed states) by comparison to data measured without buffers that MES, MOPS, and TRIS reagents did not alter the sorption behavior of Ni and Cs. The initial concentrations of Ni and Cs introduced into the system were always sufficiently high to neglect the content of Cs and Ni naturally present in bentonite; the added metal ions concentrations were higher than 90 and 99% of the natural content for Ni and Cs, respectively. Experiments were performed either in air atmosphere or in an inert gaz glovebox (N_2). In air atmosphere, the pH range studied was limited to values below 7.8 to avoid any precipitation of carbonate phases of Ca and Mg. The results showed no significant differences when CO_2 is present or not; this indicates that carbonates have not a significant influence in the experimental conditions of this study. Therefore, no distinction was made in the figures between the experiments performed in the presence or absence of CO_2.

Compacted State. A scheme of the methodology is given in Figure 1. To control the pH value of the bentonite porewater, a preequilibration of the aqueous and solid phases was necessary. This was done in the dispersed state (S/L = 10 kg/m^3). After stabilization of the pH value (it varies not more than 0.05 pH unit for 1 day), the solution was removed and replaced by a fresh one. The procedure was repeated until the equilibrium conditions were reached. Then, the solid and liquid phases were separated at 0.2 μm, the solid was dried at 35 °C, crushed, and sieved at 63 μm.

The consolidation of the preequilibrated bentonite was realized in PEEK capillaries of about 3 mm in length with 1 mm internal diameter. A small amount of bentonite was intoduced into the capillary at one extremity while the other was blocked. The bentonite was then compacted manually using a 1 mm-diameter steel drill. This step was repeated until the capillary contained about 3−4 mg of bentonite. No filter was used at the interface between the water and the compacted material. The capillaries thus prepared were put into the corresponding external solution (3 mL) for pore saturation. After swelling, the capacity of the capillaries to compact bentonite was estimated to be equal to (776 ± 106) mm (filling height in the capillary) per gram of saturated

TABLE 2. Modeling Parameters

Bentonite Description[a]

site types	Site capacities[b]	ref
exchangeable interlayer cations ≡ X	64 meq/100 g	*11*
exchangeable interlayer cations ≡ Xa	2×10^{-3} meq/100 g	this work[e]
edge site ≡ $S^{1s}OH$	1.7 μmol/g	*13,18*
edge site ≡ $S^{1w}OH$	33.6 μmol/g	this work
edge site ≡ $S^{2}OH$	33.6 μmol/g	
Site ≡ S−OH[c]	0.11 μmol/g	

Water/Solid Equilibrium

reaction	logK_{int} (this work) dispersed bentonite	logK_{int} (this work) compacted bentonite	LogK_{int} (reference study)	
$\equiv S^{1w(s)}OH \rightleftarrows \equiv S^{1w(s)}O^- + H^+$		−7.9	−7.9	
$\equiv S^{1w(s)}OH + H^+ \rightleftarrows \equiv S^{1w(s)}OH_2^+$		4.5	4.5	*13*
$\equiv S^{2}OH \rightleftarrows \equiv S^{2}O^- + H^+$		−10.5	−10.5	
$\equiv S^{2}OH + H^+ \rightleftarrows \equiv S^{2}OH_2^+$		6	6	
$\equiv SOH \rightleftarrows \equiv SO^- + H^+$		−4.7		this work
$K^+ + \equiv X(a)Na \rightleftarrows \equiv X(a)K + Na^+$		0.6	0.6	*27*
$Mg^{2+} + 2 \equiv X(a)Na \rightleftarrows \equiv X(a)_2Mg + 2Na^+$		0.34	0.34	
$H^+ + \equiv X(a)Na \rightleftarrows \equiv X(a)H + Na^+$		0	0	
$Ca^{2+} + 2 \equiv X(a)Na \rightleftarrows \equiv X(a)_2Ca + 2Na^+$		0.4	0.4	*18*
$CaCl^+ + \equiv X(a)Na \rightleftarrows \equiv X(a)CaCl + Na^+$		2.5	2.5	
$CaOH^+ + \equiv X(a)Na \rightleftarrows \equiv X(a)CaOH + Na^+$		2.5	2.5	

Sorption Reactions

element	reaction	logK_{int} (this work) dispersed bentonite	logK_{int} (this work) compacted bentonite	LogK_{int} (reference study)	
Cs	$Cs^+ + NaX \rightleftarrows CsX + Na^+$		1.65	1.65	*11*
	$Cs^+ + NaXa \rightleftarrows CsXa + Na^+$		6		this work
Ni	$Ni^{2+} + 2NaX \rightleftarrows NiX_2 + 2Na^+$		0.49	0.49	*13*
	$Ni^{2+} + \equiv S^{1w}OH \rightleftarrows \equiv S^{1w}ONi^+ + H^+$	−3.1	−3.6	−3.1	
	$Ni^{2+} + \equiv S^{1s}OH \rightleftarrows \equiv S^{1s}ONi^+ + H^+$		n.c.[d]	−0.1	
	$Ni^{2+} + \equiv SOH \rightleftarrows \equiv SONi^+ + H^+$		1.3		this work

[a] The characteristics of all edge sites are given in refs 13 and 18. Ref "This work" is associated to site S−OH 0.11 μmol/g. [b] Clay content of 84% (*11*). [c] Site considered only for Ni. [d] Not considered. [e] Site considered only for Cs. ≡ $S^{1w(s)}OH$ means ≡ $S^{1w}OH$ or ≡ $S^{1s}OH$ surface sites. ≡X(a) means ≡X or ≡Xa exchange sites.

bentonite. Then, after a contact time of at least 3 days, three types of experiments were conducted in parallel:

(1) The goal of the first series of experiments was to define, in the compacted state, the liquid and solid phases for the determination of the solid-to-liquid ratio, S/L. In this study, the liquid phase, or the pore water refers to the free water, i.e., the water not bound to bentonite. This pore water volume (θ_p) was probed using Tc(VII) and I(−I) (*16*). It was determined only at pH 7.8 for high concentrations (10^{-5}−10^{-4} M of Tc-(VII) and 10^{-3} M of I(−I)) where the adsorption of the anions can be neglected. The pore volume, composed of the bound + free water, is determined using HTO tracer (θ_{HTO}). It was additionally assessed by drying saturated and compacted bentonite at 105 °C (θ_{105}). θ_{HTO} and θ_{105} were determined for all pH values. The porosity was defined in this work by the volume of porewater (in 10^{-3} m^3) per kilogram of dry MX-80 bentonite. The mass of dry bentonite referred to the mass without the bound water, i.e., the S/L ratio corresponds to $\theta_{HTO}{}^{1-}$ 10^3 kg/ m^3.

(2) The second series gives the equilibrium state of the system when the sorption equilibrium (between the contaminant and compacted bentonite) is reached. It is characterized by the pH value and the composition of major (Na, K, Mg, Ca) and minor (Al, Si, Fe) ions in the external solution.

(3) The third series implies the measure of the sorption data either at equilibrium or as function of the contact time (between the compacted material and the solution). After a contact time of *x* days, the saturated bentonite in the capillaries was pushed out, the first part of the compacted material was removed (about 0.3 mm in height), and the material was weighted (m_{tot}). Then, it was dried at 105 °C (determination of θ_{105}) or mixed with 0.1 M HCl at a solid-to-solid ratio of 1 kg/ m^3 for analysis of the total activity in the solid (A_{tot}; determination of θ_p, θ_{HTO}, and sorption data). The activity in the external solution was also measured (A_f).

The activity in the porewater in Bq for a given sample is as follows:

$$A_p = \frac{m_{tot}.\theta_p.A_f}{(1 + \rho_{H_2O}\theta_{HTO})} \quad (1)$$

with m_{tot} in kg and A_f in Bq/L. The volumic mass of water (ρ_{H_2O}) is supposed to be equal to 1×10^3 kg/m^3.

For the experiments conducted with Tc(VII) and I(−I), $Ap = A_{tot}$. For the sorbed elements, the Kd value (in 10^{-3} m^3/kg) can be derived according to the following relation:

$$K_d(C) = \frac{A_{tot} - A_p}{A_p}.\theta_p \quad (2)$$

with A_{tot} in Bq.

For each Kd value, at least three experiments were performed. The Figures give the average values together with the standard deviations.

Dispersed State. All experiments were conducted in polyethylene tubes for S/L ratios varying from 0.5 to 10 kg/ m^3. A preequilibration of the system was performed according to the methodology presented for the compacted state. Then, the element and the corresponding tracer were introduced

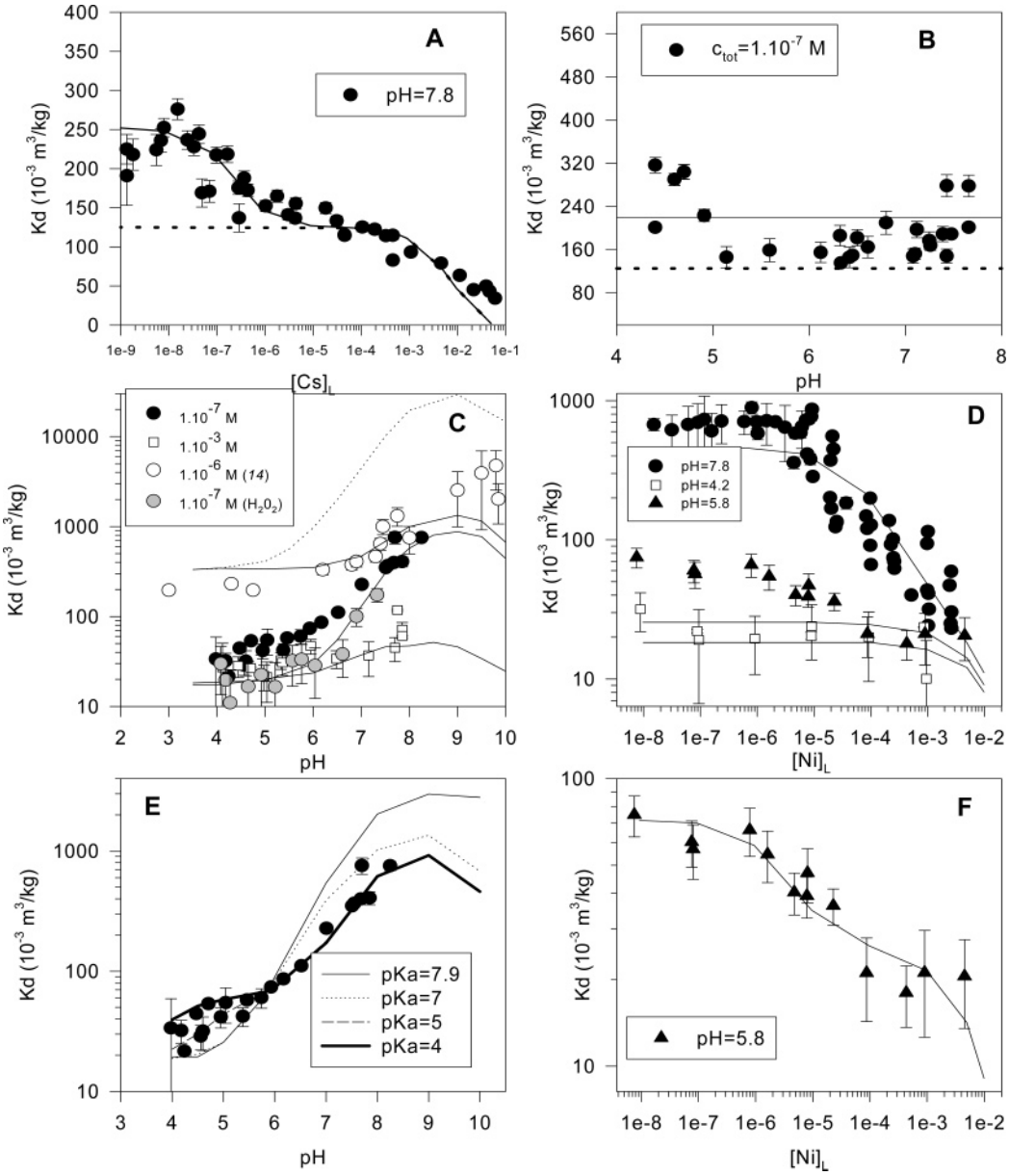

FIGURE 2. Sorption of Cs (A,B) and Ni (C−F) on bentonite in the dispersed state.Sorption isotherm (A) and sorption edge (B) measured for Cs. The calculation is made with (solid line) or without (dashed line) considering the exchangeable interlayer cations ≡Xa (see Table 2). Sorption edges (C,E) and sorption isotherms (D,F) measured for Ni. (O) Data obtained in simplified conditions (*15*); (gray circle) data measured with MX-80 bentonite treated with H_2O_2. The calculation in Figures C and D is based on the model of Bradbury and Baeyens (*13*) with (dashed line) or without (solid lines) the strong site (see Table 2). For Figures E, F, the site ≡S−OH is considered (see Table 2 and text).

in the suspension at the desired concentration. The suspensions were stirred for 7 days to reach equilibrium. Studying the sorption kinetics, this time was found to be sufficient to reach equilibrium. The solid phase was separated from the aqueous one by centrifugation for 30 min at 11 000 g. Aliquots of the supernatant were analyzed to derive the distribution coefficients using the following expression:

$$K_d(D) = \frac{A_{tot} - A_L}{A_L} \times \frac{L}{S} \quad (3)$$

where A_{tot} is the total activity added to the system (Bq), A_L is the equilibrium activity in the liquid phase (Bq), and S/L the solid-to-liquid ratio in 10^3kg/m^3.

Analytical Methods. A PQ-Excel ICP-MS (VG-Elemental) was used to analyze the major and minor cations (see Table 1). HTO, Cs (^{137}Cs), and Ni (^{63}Ni) analysis were performed by liquid scintillation counting using a Packard 2550 TR/AB liquid scintillation analyzer. The scintillation cocktail was ULTIMA GOLD AB (Packard).

Modeling. The objective is to use the data measured in the dispersed state to define an operational model allowing us to predict the retention in the compacted state. The basic assumption in both cases is that Cs and Ni sorb predominantly on the montmorillonite fraction of MX-80 bentonite.

The minerals dissolution is considered indirectly by introducing the measured concentration of Si, Al, and Fe in the solution (Table 1). At the solid/water equilibrium, the composition of the exchange sites as well as the speciation of the surface sites are calculated for the solution composition (Table 1) using the parameters given in Table 2.

The acid−base properties of edge sites is still a matter of discussion in the literature (*17*). In the present study, the simplified two-p*K* nonelectrostatic model from Bradbury et

al. (*13*) is used. Although it has no real physical meaning (*18*), it remains an "operational" model tested with many radionuclides (see references quoted). In the model, the electrostatic term is not explicitely represented. Either it is of significance importance and the pH-dependent Coulombic contribution is included in the interaction constants (*19*) or it can be ignored (*18*)

For compacted and dispersed states, sorption is described by pH-dependent interaction with clay edges and by the cation exchange in the interlayer and on the basal plane surfaces. The parameters used to describe the interaction between Ni and Cs and montmorillonite are included in Table 2. Except for the major element exchange, the competition of metallic impurities with Cs and Ni for sorption sites is not considered. First, the amount of mobilized metallic impurities from MX-80 bentonite is not higher than 10^{-7} mol/g (*15*). Second, the preequilibrium step following the batch procedure (Figure 1) is expected to reduce impurities to even lower values. Third, considering the S/L ratios explored in the present study, the number of sorption sites is much higher than the concentration of impurities.

The Phreeqc code was used to model the sorption results using the Llnl.dat database to calculate the speciation in aqueous solution (*20*). For the kinetic experiments, the sorption model was coupled with a transport model considering a diffusion process. For the transport part, the only fitting parameter was the diffusion coefficient.

Results and Discussion

System Characterization. *Porosity Characterization in the Compacted State.* θ_{HTO} and θ_{105} were found similar irrespective of the pH value. The pore volume determined by drying at 105 °C amounts to $(0.41 \pm 0.05) \times 10^{-3}$ m^3/kg. This value appears sligthly lower than that determined with HTO $(0.49 \pm 0.03) \times 10^{-3}$ m^3/kg. The dry density of bentonite amounts to 1100 ± 60 kg/m^3.

The free pore water volume probed by TcO_4^- and I^- was found to be equal to $(0.24 \pm 0.04) \times .10^{-3}$ m^3/kg independent of the concentration and choice of the anion. Due to the anionic exclusion phenomenon, the anions access neither to the water in the double layers associated with external surfaces of the clay stacks, nor in the interlayer space (*16*). The distribution free/bound water appears, therefore, in the proportions 49:51%. Considering a value of 0.3 nm for one water layer, the different specific surface areas of montmorillonite (i.e., 30 and 8.5 m^2/g for the external basal and edge surfaces, respectively and 750 m^2/g for the interlayer surface area) (*18*) and 2−2.5 (*21*) and 2−3 (*21*, *22*) water layers for the external and internal surfaces, respectively, one would calculate a free porosity value of $\theta_p = 0.18 \pm 0.06$ L/kg. The prediction appears coherent, at least within experimental errors, with the experiment.

The S/L ratio corresponding to θ_p^{-1} amounts to 4200 kg/m^3. This value is supposed to be constant in the pH range investigated (*4*−*9*).

Water/Solid Equilibrium. Table 1 summarizes the characteritics of the solution (pH, major and minor concentrations) after reaching sorption equilibrium for dispersed and consolidated states. A slight increase in the ionic strength is oberved in the compacted state. This may be explained by a sligth evaporation of the external solution after the equilibrium period. For the minor elements, the concentration remains nearly constant, irrespective of the system considered. The measured concentrations are similar to values measured for equilibrium of purified montmorillonite with water (*12*, *17*).

Sorption Studies. *Dispersed State*. Experimental results for Cs and Ni are given in Figures 2. Model parameters describing the interaction of Cs and Ni with montmorillonite are already available in the literature. The works of Bradbury and Baeyens (for Ni) (*12*, *13*) and Hurel et al. (for Cs) (*11*) performed under well-controlled conditions (simplified medium, purified Na-montmorillonite) with Swy-1 and MX-80 Na-montmorillonite, respectively, were chosen as references for this study. For Cs, the lines in Figure 2 correspond to the calculation made considering an interaction governed by the exchange sites using only the published exchange constant (*11*). The prediction agrees to the experimental data for equilibrium solution concentrations (C_L) above 10^{-6} M. At lower concentrations, the prediction underestimates the sorption by a factor of about 0.6. This indicates the existence of a second interacting site governing Cs sorption for trace concentrations. According to the literature, this may be explained by the interaction of Cs with edge sites (*11*, *23*). However, the pH-edge measured for trace concentrations (Figure 2B) shows that the interaction is not affected by the change in pH. The mechanism associated to this second site must also be a cation exchange mechanism with interlayer cations. This could be the result of different binding energies of Cs in the interlayer due to different substitutions in octahedral and tetrahedral sites. Alternatively, it may also be due to the existence of a low amount of another clay mineral in MX-80 bentonite. Under a quantitative point of view, the interaction of Cs with this new exchange site must be stronger than that presented by montmorillonite (i.e., ≡X site, Table 2). The new site (i.e., ≡Xa site, Table 2) is introduced in the model with the parameters given in Table 2. It shall be noted that the parameters are applicable only for the conditions of the present study.

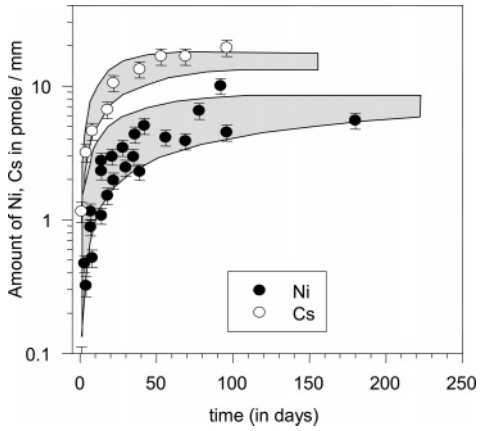

FIGURE 3. Sorption kinetics of Ni (●) and Cs (○) on compacted bentonite. Cs: $C_{tot} = <5 \times 10^{-9}$ M; pH 7.8; Ni: $C_{tot} = 5 \times 10^{-8}$ M; pH 7.8. The gray zones correspond to the simulation made with the PHEEQC transport code considering a diffusive transport (see text).

The sorption edge data and isotherms obtained for Ni are presented in Figure 2C,D together with the published sorption edge data obtained with (MX-80) Na-montmorillonite in $NaNO_3$ 0.05 M (*15*) (Figure 2C). The latter series is used to test the model of Bradbury and Baeyens obtained for montmorillonite extracted from Swy-1 bentonite (*13*). As shown by the dashed line in Figure 2C, the model overestimates the retention by more than 1 order of magnitude when the surface complexation mechanism dominates (pH > 5, trace concentrations). This deviation can be explained with the parameters of Bradbury and Baeyens considering the presence of a strong competiting agent, like Zn, at a concentration of 10^{-5} M. Such a concentration was not detected and a competition effect is, therefore, not expected. The agreement becomes better if the interaction of Ni with the strong site is entirely negected. This modified model also allows us to describe the data measured with bentonite and the synthetic groundwater (SGW) (solid lines in Figure 2C,D). The results may indicate that the strong site present on montmorillonite extracted from Swy-1 bentonite (Swy-1

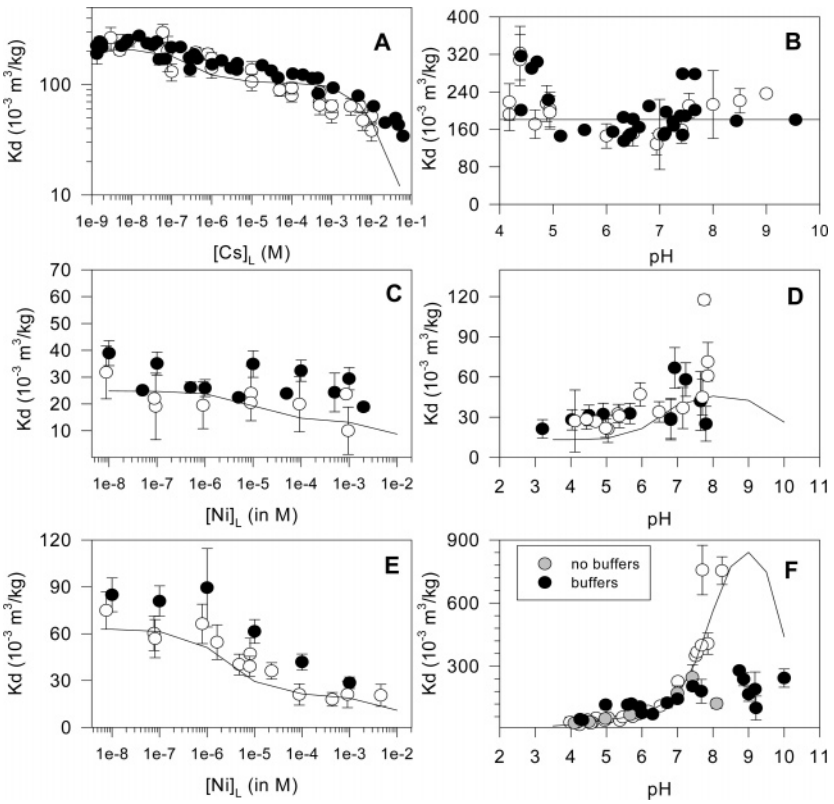

FIGURE 4. Comparison between dispersed and consolidated states for Cs (A,B) and Ni (C−F). Sorption isotherm (A) and soption edge (B) measured for Cs. Sorption isotherms at pH 4.2 (C) and 5.8 (E) and sorption edges for $C_{tot(L)} = 1 \times 10^{-3}$ M (D) and 1×10^{-7} M (F) measured for Ni in the compacted (solid points) and dispersed (open points) states. The solid lines correspond to the prediction made with the model obtained for dispersed bentonite (see Table 2).

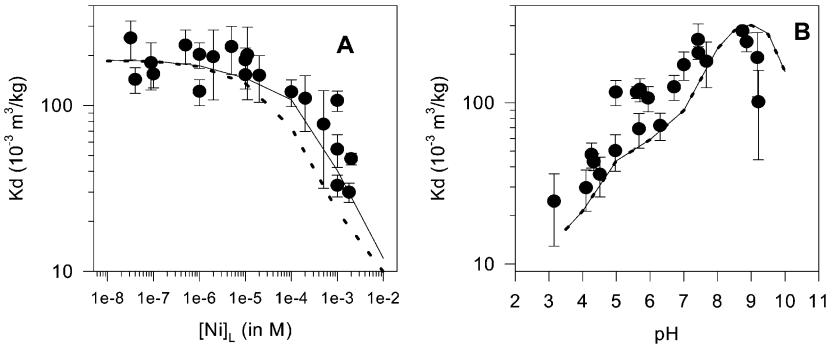

FIGURE 5. Sorption isotherm (A) (pH 7.8) and sorption edges (B) ($C_L = 1 \times 10^{-7}$ M) measured for Ni in the compacted state. The lines correspond to model adapted to the compacted medium considering either a diminution of the interaction constant (solid line, logK = −3.6) or a diminution of the number of sites (dashed line, 0.046 μmol/g).

montmorillonite) is not present on the clay material extracted from MX-80 bentonite (MX-80 montmorillonite).

A detailed examination of the data reveals however a slight disagreement between the model and the experience. In the pH range between 4 and 6 for trace concentrations, the model underestimates the retention. This may be explained by a pH-dependent interaction of Ni with another site. An estimation of the parameters associated to this interaction were obtained as follows: the apparent deprotonation constant (ka) was fixed while the number of sites and the interaction contant were fitted using the isotherm measured at pH 5.8 (Figure 2F). The pH-edge for trace concentration was then calculated and compared with the experimental data (Figure 2E). This was done for log ka values varying from −8 to −4 (see Figure 2E). The best agreement is found with the parameters given in Table 2. The pK_a value appears lower than those generally found for mineral surface sites. MX-80 bentonite contains about 0.4% in weight of organic matter (*24*). Organic matter, and particularly carboxylate groups, could be reponsible for this interaction. This assumption is confirmed by the data measured with bentonite treated with H_2O_2: between pH 4 and pH 7; the calculation made with the modified model of Bradbury and Baeyens (*13*) agrees with the experiment without considering the interaction of Ni with a secondary phase (Figure 2C, gray symbols).

In conclusion, the cationic exchange mechanism dominates the sorption for Ni concentrations above 10^{-4}M and pH < 4. Organic matter is the dominant interacting phase for trace concentrations and pH values varying from 4 to 6. Finally, in conditions relevant to nuclear waste disposal (pH > 7, trace concentrations) (*25*), the sorption is governed by a surface complexation mechanism with edge surface sites. Montmorillonite appears in this case to be the dominant interacting phase.

Compacted State. Kinetic. The design can be decomposed into two systems: the external solution in equilibrium with the atmosphere and the compacted medium where the porewater is locally in equilibrium with bentonite for a high solid-to-liquid ratio. Before the addition of Cs or Ni, and according to the methodology given in Figure 1, the whole system is considered in equilibrium, i.e., the water of the external solution (in equilibrium with the atmosphere) has the same composition as the free pore water. In the presence of Cs or Ni, the equilibrium is disturbed by the sorption of the element on bentonite. Two processes need to be considered:

(1) The diffusion of Cs or Ni from the external solution to the porewater and the sorption of the element on bentonite.

(2) The reequilibration of the pore water composition with respect to the water of the external solution after the sorption reaction.

In the conditions of the study, the volume of the external solution is much higher than the volume of the porewater (V(external solution)/V(porewater) > [2×10^6]). Therefore, the composition of the external solution does not vary during the sorption process. The equilibration process was followed by analyzing the temporal evolution of the content of Ni or Cs in the compacted system (i.e., pore volume + bentonite). The sorption equilibrium is considered to be reached when it does not vary anymore with contact time.

This is illustrated in Figure 3 for Ni and Cs. The amount of Ni and Cs in the capillaries increases as the contact time increases till a plateau is reached after about 40 days for both cations. The gray zones corespond to the simulation made with the PHEEQC code. The calculation takes the variation of the mass of saturated bentonite in the different capillaries ($m_{tot} = 3.9 \pm 0.5$ and 4.0 ± 1.0 for Cs and Ni, respectively) and the uncertainty associated to the consolidation capacity of the capillaries (776 ± 106 mm per gram of saturated bentonite) into account. The increase in concentration is well described by a diffusion process of Ni, Cs from the external solution to the compacted clay medium with an effective diffusion coefficient of 5×10^{-10} m^2/s for both cations. At equilibrium, in the case of Ni, a decrease of the retention capacity of bentonite, as compared to that determined in the dispersed state, is needed for a good agreement (see next section).

Based on these results, equilibration times were fixed at 2 and 3 months for Cs and Ni, respectively.

Data at Equilibrium. The experimental data measured for Cs with the compacted material are given in Figure 4A,B together with the data measured in the dispersed state. A good agreement is found between both series of experiments. As indicated by the solid lines, the model derived from the dispersed state describes the data in the compacted state. The cation exchange capacity and the constants characterizing the interaction appear, therefore, not significantly affected by the consolidation.

Sorption edges and sorption isotherms obtained for Ni in the compacted state are displayed in Figure 4C−F. The results obtained in the presence and absence of buffers are nearly identical. As it is the case in the dispersed state (*12*), the buffers used in (*12*) do not alter the sorption behavior of Ni on compacted bentonite. When the cation exchange mechanism (Figure 4C,D) and/or the interaction of Ni with organic surface sites (Figure 4E) dominates, the agreement between dispersed and consolidated states is good.

On the other hand, when the surface complexation mechanism with edge sites dominates, a significant deviation between the model and the experiment is observed (Figure 4F). Quantitatively, this may be explained by a modification of the interaction constant or by a diminution of the number of sites. Both assumptions were tested in Figure 5, and the results show that the first assumption is more reliable. An interesting consequence of this decrease is that even if the clay portion of MX-80 bentonite remains the predominant interacting phase, organic matter, despite its low content, becomes a significant interacting phase in the compacted system in conditions relevant to nuclear waste disposal (it contributes to about 20% of the total sorption capacity of bentonite). The origin of the decrease appears unclear. It may be explained either by a modification of the complexed species in the compacted species (a change of the intrinsic binding constant) or by a modification of the electrostatic term contribution in the conditional constant. The origin of the effect could arise from the interaction between edge surfaces in the compacted state (*26*). However, further experiments are necessary to understand the exact nature of the consolidation effect on the retention.

Acknowledgments

We thank the French National Agency for Radioactive Waste Management (ANDRA) for providing us the bentonite and for their financial support. X.K. WANG is thanked for its experimental contribution concerning the measure of sorption data in the dispersed state. Financial support for X.K. WANG from the French Research Ministry is gratefully acknowledged.

Literature Cited

(1) Nowak, E. J. In *Scientific Basis for Nuclear Waste Management II;* Northrup, C. J. M., Jr., Ed.; Elsevier: New York, 1980; p 403.

(2) Bradbury, M. H.; Baeyens, B. *Near field sorption data bases for compacted MX-80 bentonite for performance assessment of a high-level radioactive waste repository in opalinus clay host rock*, PSI Report N. 03-07; PSI: Oakbrook Terrace, IL, 2003.

(3) Yu, J.-W.; Neretnieks, I. *Diffusion and sorption properties of radionuclides in compacted bentonite*, SKB report TR 97-12; SKB: Stockholm, 1997.

(4) Bourg, I. C.; Bourg, A. C. M.; Sposito G. Modeling diffusion and adsorption in compacted bentonite: A critical review. *J. Contam. Hydro.* **2003**, *61*, 293.

(5) Bradbury, M. H.; Baeyens, B. A. *Comparison of apparent diffusion coefficients deduced from diffusion experiments in compacted Kunigel V1 bentonite with those derived from batch sorption measurements: A case study for Cs(I), Ni(II), Sm(III), Am(III), Zr(IV) and Np(V)*, PSI Report N. 03-02, Nagra NTB 02-17; PSI: Oakbrook Terrace, IL, 2003.

(6) Ochs, M.; Lothenbach, B.; Shibata, M.; Sato, H.; Yui, M. Sensitivity analysis of radionuclide migration in compacted bentonite: a mechanistic model approach. *J. Contam. Hydro.* **2003**, *61*, 313.

(7) Ochs, M.; Boonekamp, M.; Wanner, H.; Sato, H.; Yui, M. A quantitative model for ion diffusion in compacted bentonite. *Radiochim. Acta* **1998**, *82*, 437.

(8) Eriksen, T. E.; Jansson, M. *Diffusion of I^- Cs^+ and Sr^{2+} in compacted bentonite. Anion exclusion and surface diffusion*, SKB report TR 96-16; SKB: Stockholm, 1996.

(9) Oscarson, D. W.; Hume, B. H.; King, F. Sorption of cesium on compacted bentonite. *Clay Clay Miner.* **1994**, *42*, 731.

(10) Muurinen, A.; Penttilä-Hiltunen, P.; Rantanen, J. Diffusion mechanisms of strontium and cesium in compacted sodium bentonite. *Mater. Res. Soc. Symp. Proc.* **1987**, *84*, 804.

(11) Hurel, C.; Marmier, N.; Séby, F.; Giffaut, E.; Bourg, A. C. M.; Fromage, F. Sorption behaviour of caesium on a compacted bentonite sample. *Radiochim. Acta* **2003**, *90*, 1.

(12) Baeyens, B.; Bradbury, M. H. A mechanistic description of Ni and Zn sorption on Na-montmorillonite. Part I: Titration and sorption measurements. *J. Contam. Hydrol.* **1997**, *27*, 199.

(13) Bradbury, M. H.; Baeyens, B. A mechanistic description of Ni and Zn sorption on Na-montmorillonite. Part II: Modelling. *J. Contam. Hydrol.* **1997**, *27*, 223.

(14) Kunze, G. W.; Dixon, J. B. Pretreatment for mineralogical analysis. In *Methods of Soil Analysis: Part I, Physical and Mineralogical Methodologies*, Agronomy Monograph No 9, 2nd ed; Klute A., ed.; American Society of Agronomy: Madison, WI, 1986; p91.

(15) Hurel, C. Thèse de doctorat. Rétention d'éléments trace sur une bentonite: étude expérimentale et modélisation. Université de Nice Sophia Antipolis, 2002.

(16) Bradbury, M. H.; Baeyens, B. Porewater chemistry in compacted re-saturated MX-80 bentonite. *J. Contam. Hydrol.* **2003**, *61*, 329.

(17) Duc, M.; Gaboriaud, F.; Thomas, F. Sensitivity of the acid−base properties of clays to the methods of preparation and measurement. 1. Literature review. *J. Colloid Interface Sci.* **2005**, *289*, 139. Duc, M.; Gaboriaud, F.; Thomas, F. Sensitivity of the acid−base properties of clays to the methods of preparation and measurement. 2. Evidences from continuous potentiometric titrations. *J. Colloid Interface Sci.* **2005**, *289*, 148.

(18) Tournassat, C.; Ferrage, E.; Poinsignon, C.; Charlet, L. The titration of clay minerals I. Discontinuous backtitration technique combined with CEC measurements. *J. Colloid Interface Sci.* **2004**, *273*, 224. Tournassat, C.; Greneche, J.-M; Tisserand, D.; Charlet, L. The titration of clay minerals II. Structural based model and implications on clay reactivity. *J. Colloid Interface Sci*. **2004**, *273*, 234.

(19) Bradbury, M. H.; Baeyens, B. Sorption of Eu on Na- and Ca-montmorillonites: Experimental investigations and modelling with cation exchange and surface complexation. *Geochim. Cosmochim. Acta* **2002**, *66*, 2325.

(20) Parkhurst, D. L.; Appelo, C. A. J. *User's Guide to PHREEQC (Version 2)—A Computer Program for Speciation, Batch Reaction, One-Dimensional Transport, and Inverse Geochemical Calculations*, Report 99-4259; U.S. Geological Survey: Denver, CO, 1999; pp 1−326.

(21) Pusch, R. *The microstructure of MX-80 clay with respect to its bulk physical properties under different environmental conditions*, SKB report TR 01-08; SKB: Stockholm, 2001.

(22) Torikai, Y.; Sato, S.; Ohashi, H. In *Scientific Basis for Nuclear Waste Management XVIII;* Murakami, T., Ewing, R. C., Eds.; Elsevier: New York, 1995; p 353.

(23) Poinssot, C.; Baeyens, B.; Bradbury, M. H. Experimental and modelling study of the Cs sorption on illite. *Geochim. Cosmochim. Acta* **1999**, *63*, 3217.

(24) Müller-Vonmoos, M.; Kahr, G. *Mineralogische Untersuchungen von Wyoming Bentonite MX-80 und Montigel*, Nagra NTB 83−13, Nagra: Wettingen Switzerland, 1983.

(25) Gaucher, E.; Robelin, C.; Matray, J. M.; Négrel, G.; Gros, Y.; Heitz, J. F.; Vinsot, A.; Rebours, H.; Cassagnabère, A.; Bouchet, A. ANDRA underground research laboratory: interpretation of the mineralogical and geochemical data acquired in the Collovian-Oxfordian formation by investigative drilling. *Phys. Chem. Earth* **2004**, *29*, 55.

(26) Lagaly, G.; Ziesmer, S. Colloid chemistry of clay minerals: the coagulation of montmorillonite dispersion. *Adv. Colloid Interface Sci.* **2003**, *100*, 105.

(27) Bradbury, M. H.; Baeyens, B. *Porewater chemistry in compacted re-saturated MX-80 bentonite: Physico-chemical characterisation and geochemical modelling*, PSI Report N. 02-10, Nagra NTB 01-08; PSI: Oakbrook Terrace, IL, 2002.

Received for review December 12, 2005. Revised manuscript received April 6, 2006. Accepted May 30, 2006.

ES052483I